Regular Article

LYMPHOID NEOPLASIA

The role of HTLV-1 clonality, proviral structure, and genomic integration site in adult T-cell leukemia/lymphoma

Lucy B. Cook,[1] Anat Melamed,[1] Heather Niederer,[1] Mikel Valganon,[2,3] Daniel Laydon,[1] Letizia Foroni,[2,3] Graham P. Taylor,[4] Masao Matsuoka,[5] and Charles R. M. Bangham[1]

[1]Section of Immunology, Wright-Fleming Institute, Imperial College, London, United Kingdom; [2]Imperial Molecular Pathology Laboratory, Imperial College Healthcare NHS Trust and Academic Health Sciences Centre, Hammersmith Hospital, London, United Kingdom; [3]Centre for Haematology, Faculty of Medicine, Imperial College, Hammersmith Hospital, London, United Kingdom; [4]Section of Virology, Wright-Fleming Institute, Imperial College, London, United Kingdom; and [5]Institute for Viral Research, Kyoto University, Kyoto, Japan

Key Points

- Adult T-cell leukemia (ATL) does not, as previously believed, result from the oligoclonal proliferation caused by HTLV-1 infection.
- In both ATL patients and those with nonmalignant infection, the HTLV-1 provirus preferentially survives in vivo in acrocentric chromosomes.

Adult T-cell leukemia/lymphoma (ATL) occurs in ~5% of human T-lymphotropic virus type 1 (HTLV-1)–infected individuals and is conventionally thought to be a monoclonal disease in which a single HTLV-1$^+$ T-cell clone progressively outcompetes others and undergoes malignant transformation. Here, using a sensitive high-throughput method, we quantified clonality in 197 ATL cases, identified genomic characteristics of the proviral integration sites in malignant and nonmalignant clones, and investigated the proviral features (genomic structure and 5′ long terminal repeat methylation) that determine its capacity to express the HTLV-1 oncoprotein Tax. Of the dominant, presumed malignant clones, 91% contained a single provirus. The genomic characteristics of the integration sites in the ATL clones resembled those of the frequent low-abundance clones (present in both ATL cases and carriers) and not those of the intermediate-abundance clones observed in 24% of ATL cases, suggesting that oligoclonal proliferation per se does not cause malignant transformation. Gene ontology analysis revealed an association in 6% of cases between ATL and integration near host genes in 3 functional categories, including genes previously implicated in hematologic malignancies. In all cases of HTLV-1 infection, regardless of ATL, there was evidence of preferential survival of the provirus in vivo in acrocentric chromosomes (13, 14, 15, 21, and 22). (*Blood.* 2014;123(25):3925-3931)

Introduction

Human T-lymphotropic virus type 1 (HTLV-1) causes adult T-cell leukemia/lymphoma (ATL) in approximately 5% of HTLV-1–infected individuals. A further ~5% of carriers develop an aggressive myelopathy known as HTLV-1–associated myelopathy (HAM) or other inflammatory diseases such as polymyositis. It remains uncertain why a minority develop aggressive clinical disease, typically decades following asymptomatic infection, whereas most infected individuals remain lifelong healthy carriers. The Shimoyama classification of ATL[1] contains 4 subtypes: acute, lymphoma, chronic, and smoldering. These subtypes differ in the response to treatment and overall survival, but little is known about either viral or host molecular determinants of disease. Several host cytogenetic or molecular defects have been described, but no recurrent genetic lesions have been identified.

The major predictor of clinical disease is the proviral load (PVL), the percentage of HTLV-1–infected peripheral blood mononuclear cells (PBMCs). The PVL remains relatively constant over years within an individual, rising slowly over decades.[2] However, the PVL varies widely between patients, ranging from <0.001% PBMCs to >100% (ie, >100 copies per 100 PBMCs); the risk of disease rises in carriers with a PVL >4% in Japan[3] and in those with a PVL >10% in the United Kingdom.[4] Nonetheless, there is overlap in the range of PVL seen between patients with disease and those that remain lifelong asymptomatic carriers, making individual patient prognosis difficult.

HTLV-1 appears to persist in chronic infection chiefly by mitotic proliferation of infected CD4$^+$ T cells, although the ratio of this mitotic spread to de novo infection[5] has not been rigorously estimated. Each clone of HTLV-1–infected cells can be identified by its particular integration site of the HTLV-1 provirus in the host genome[6]; the daughter cells of each clone share the same genomic integration site, and the frequency of these cells defines the abundance of a given clone. A majority of naturally infected cells in nonmalignant infection contain a single integrated provirus.[7]

ATL is characterized by monoclonal proliferation of CD4$^+$CD25$^+$ tumor cells. For many years, it has been believed that ATL arises following a steady progression from polyclonal infection of CD4$^+$ T cells to an oligoclonal expansion and, many years later, following a series of undefined genetic or epigenetic events, malignant transformation of a previously abundant clone to a monoclonal tumor. However, there are indications that HTLV-1 clonality in ATL may be

Submitted February 1, 2014; accepted April 3, 2014. Prepublished online as *Blood* First Edition paper, April 15, 2014; DOI 10.1182/blood-2014-02-553602.

A.M., H.N., and M.V. contributed equally to this study.

The online version of this article contains a data supplement.

The publication costs of this article were defrayed in part by page charge payment. Therefore, and solely to indicate this fact, this article is hereby marked "advertisement" in accordance with 18 USC section 1734.

more complex. One or more abnormally abundant clones may underlie the largest, putatively malignant clone,[6] and there are reports of "clonal succession" in which a malignant clone spontaneously regresses and an independent clone proliferates in its place.[8]

HTLV-1 expresses a transcriptional transactivator protein, Tax, which activates transcription of the HTLV-1 provirus and of many host genes[9]. Because Tax can immortalize rodent cells in vitro and Tax transgenic mice develop tumors, it has been widely accepted that Tax plays a role in leukemogenesis. This hypothesis is supported by the observations that Tax promotes DNA replication and cell-cycle progression, causes structural damage to host DNA, and inhibits DNA repair and cell-cycle checkpoints.[9] Tax expression is lost in ~40% of ATL cases, probably under selection from the strong anti-Tax cytotoxic T-lymphocyte (CTL) response,[10] but the relation between Tax expression and ATL subtype and progression is unclear. There is also increasing evidence that another HTLV-1 gene, *HBZ*, plays a critical part in leukemogenesis.[9]

To summarize, the molecular mechanisms of oncogenesis of ATL, and in particular the mechanisms and role of selective oligoclonal proliferation, are incompletely understood. Here, in a large cohort of ATL patients and geographically matched asymptomatic HTLV-1 carriers, we used a quantitative high-throughput sequencing approach to test the hypothesis that the genomic environment flanking the proviral integration site is associated with malignant transformation of HTLV-1–infected clones and correlated the findings with both the clinical subtype of ATL and genetic and epigenetic modifications of the HTLV-1 provirus.

Methods

Study subjects and control cell lines

Blood or lymph node samples were donated by 221 ATL patients and 75 asymptomatic HTLV-1 carriers (ACs) from the Kumamoto region of Japan, and DNA was extracted at the Institute for Viral Research, Kyoto University, Japan, with written consent in accordance with regulations defined by the Japanese Government and Kyoto University. This study was conducted in accordance with the Declaration of Helsinki. This study was approved by the UK National Research Ethics Service (reference 09/H0606/106). The chromosomal distribution of integration sites in the present cohort was compared with the distribution in samples from 2 previously described studies: individuals with natural (nonmalignant) HTLV-1 infection from Kagoshima, southern Japan,[11,12] and cells infected with HTLV-1 in vitro.[6,13] The rodent cell line Tarl2, containing a single copy of HTLV-1, was used for quantification of PVL. ATL control cell lines T-43 (methylated) and T-48 (unmethylated) were used as methylation controls.[14]

PVL quantification

PVL was measured by quantitative polymerase chain reaction (PCR) of *tax* and *actin* genes using ABI Fast SYBR green as per the manufacturer's protocol (Applied Biosystems), using PCR primers as previously described[15] and assuming a single copy of *tax*[7] and 2 copies of *actin* per cell. Thermal cycling conditions were 95°C for 20 seconds and 40 cycles each of 95°C for 1 second followed by 60°C for 20 seconds. Standard curves were generated using serial dilutions of the cell line Tarl2, as previously described.[6,13]

Long-range PCR to identify defective proviruses

An internal control region at the 3′ end of the HTLV-1 genome was amplified for each ATL case, followed by a long-range PCR to identify defective proviruses based upon the length of the long-range PCR product as published by Tamiya et al.[16] DNA was amplified using KOD Hot Start DNA polymerase (Toyoba, Novagen). Primers for the control PCR and cycling conditions were 5′-CTCTCACAGTGGGCTCGAGA-3′ and 5′-CAAAGACGTAGAGTT GAGCAAGC-3′, 95°C for 2 minutes, 30 cycles: 95°C for 20 seconds, 59°C for 10 seconds, and 70°C for 48 seconds, followed by 70°C for 5 minutes. The primers and cycling conditions for the long-range PCR were 5′-CTTAGAGCCTCCCAGTGAAAAACATTTCC-3′ and 5′-GATG CATGGTCCTGCAAGGATAACA-3′, 95°C for 2 minutes, 30 cycles: 95°C for 20 seconds, and 66°C for 175 seconds, followed by 72°C for 15 minutes. The PCR products were electrophoresed on a 1% agarose gel with expected product size of 2.85 kb for the control PCR and 6.5 kb for a complete long-range product. A long-range product shorter than 6.5 kb defines a type 1 defective provirus; failure to amplify any long-range product identifies a type 2 defective provirus.[16]

Exon 2 and exon 3 tax gene sequencing

Tax protein is 353 amino acids in length: exon 2 provides the methionine start codon, and the remaining amino acids are derived from exon 3. Exons 2 and 3 were sequenced in ATL samples with a complete provirus. Exon 2 was amplified using PCR products from long-range PCR using Phusion high-fidelity DNA polymerase (New England Biolabs [NEB]). Primers and cycling conditions were 5′-CCTCAGCAATAAACAAACCC-3′ and 5′-CAATTG TGAGAGTACAGCAG-3′, 98°C for 30 seconds, 20 cycles: 98°C for 5 s seconds, 51.5°C for 20 s seconds, and 72°C for 10 seconds, followed by 72°C for 5 minutes. PCR products were inspected on 2% agarose gel for product length (318 bp). Exon 3 was amplified from the control long-range PCR product using Phusion high-fidelity DNA polymerase (NEB). Primers and cycling conditions were 5′- ATACAAAGTTAACCATGCTT-3′ and 5′- AGACGTCAGAGCCTTAGTCT-3′, 98°C for 30 seconds, 20 cycles: 98°C for 5 seconds, 51.5°C for 10 seconds, and 72°C for 22 seconds, followed by 72°C for 5 minutes. PCR products were inspected on a 2% agarose gel for product length (1120 bp) and sequenced by Sanger sequencing using 6 different sequencing primers to capture the entire exon (5′-ATACAAAGTTAACCA TGCTT-3′, 5′-CGTTATCGGCTCAGCTCTACA-3′, 5′-TTCCGTTCC ACTCAACCCTC-3′, 5′- AGACGTCAGAGCCTTAGTCT-3′, 5′-GGGTT CCATGTATCCATTTC-3′, and 5′- GTCCAAATAAGGCCTGGAGT-3′).

Methylation-specific PCR (MS-PCR)

MS-PCR was undertaken on ATL samples with a complete provirus but without a nonsense mutation of the *tax* gene. Takeda et al[17] showed that MS-PCR correlates with bisulfite sequencing PCR and with the methylation status of the promoter/enhancer Tax-response element-1 in the 5′ long terminal repeat (LTR). DNA was treated overnight with sodium bisulfite (Sigma) and purified using Zymo EZ Bisulfite DNA cleanup as per the manufacturer's protocol (Zymo Research). DNA was amplified by heminested PCR using JumpStart RedTaq polymerase (Sigma). Primers for the first PCR reaction for methylated DNA were 5′-TTAAGTCGTTTTTAGGCGTTGAC-3′, 5′-AAA AAAATTTAACCCATTACC-3′ and for unmethylated DNA 5′- TTAA GTTGTTTTTAGGTGTTGAT-3′, 5′-AAAAAAATTTAACCCATTACC-3′. The thermal conditions for first PCR were 94°C for 2 minutes, 35 cycles: 94°C for 30 seconds, 53°C for 30 seconds, and 72°C for 2 minutes. Primers for the hemi-nested methylated PCR were 5′-GAGGTCGTTATTTACGTCGGTT GAGTC-3′, 5′-AAAAAAATTTAACCCATTACC-3′ and unmethylated PCR primers 5′-GAGGTTGTTATTTATGTTGGTTGAGTT-3′, 5′-AAAAAAA TTTAACCCATTACC-3′. The cycling conditions for the second PCR were 94°C for 2 minutes, 30 cycles: 94°C for 30 seconds, 57°C for 30 seconds, and 72°C for 2 minutes, followed by 72°C for 5 minutes. The PCR product was inspected on a 2% agarose gel for length (428 bp). MS-PCR primers did not amplify unconverted HTLV-1 or host genomic DNA.

T-cell receptor (TCR) gene rearrangement studies

TCR-γ gene rearrangement studies were undertaken in the Imperial Molecular Pathology Laboratory, Hammersmith Hospital (London, United Kingdom) using the established BIOMED-2 protocol followed by heteroduplex analysis and/or GeneScanning. GeneScan analysis was performed on an ABI 3130 genetic analyzer using GeneMapper 4.0 (Life Technologies).

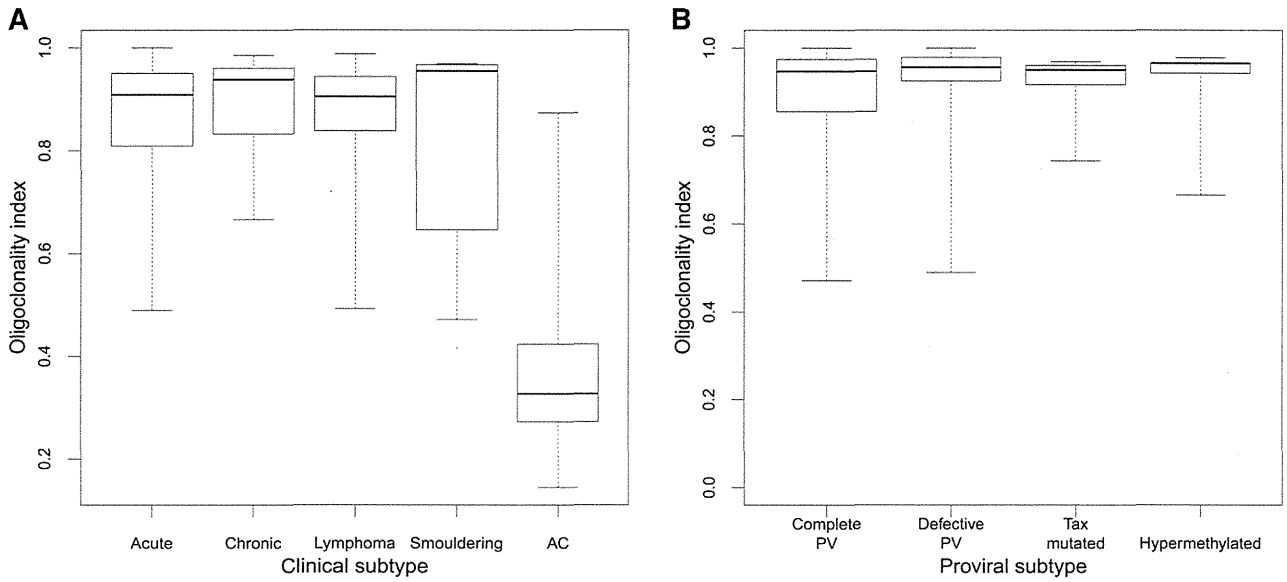

Figure 1. OCI by clinical and proviral subtype. (A) Median OCI of the ACs was 0.33 (range, 0.14-0.87), and median OCI for the ATL (all subtypes combined) was 0.91 (range, 0.47-1.0). There was no difference in OCI between ATL clinical subtypes. (B) There was no difference in OCI between the different mechanisms of proviral silencing. PV, provirus.

Integration site mapping and quantification

The high-throughput protocol for identification and quantification of proviral integration sites was carried out as previously described.[6] Mapped integration sites were compared with a set of randomly generated in silico genomic sites (n = 175 505) as previously reported.[13]

Bioinformatic annotation of genomic environment

Transcription units and cytosine guanine dinucleotide island data were retrieved from the National Center for Biotechnology Information (ftp.ncbi.nih.gov/gene/) and University of California, Santa Cruz tables, respectively. Epigenetic marks were annotated according to primary $CD4^+$ T-cell chromatin immunoprecipitation sequencing data published by Barski et al.[18] Transcription factor binding sites were obtained from published data sets (supplemental Figure 1 available at the *Blood* Web site) from chromatin immunoprecipitation sequencing experiments on primary human $CD4^+$ T cells or other primary human cells or cell lines, as previously described.[13] Cancer-associated gene data sets are defined by Sadelain et al.[19] Annotated genomic positions were compared with the integration site data using the hiAnnotator R package kindly provided by N. Malani and F. Bushman (University of Pennsylvania; http://malnirav.github.com/hiAnnotator).

Diversity estimator

The diversity estimator (DivE)[20] was used to estimate the total number of clones in addition to those observed. DivE involves fitting many mathematical models to nested subsamples of individual-based rarefaction curves. Estimates from the best-performing models are aggregated to produce the final estimate.[20] DivE requires an estimate of the number of cells in the blood; because the absolute PBMC count for each case was unknown, DivE estimates were calculated for each patient over 2 orders of magnitude of variation in the PBMC count (3×10^9/L, 50×10^9/L, and 500×10^9/L).

Statistical analysis

Statistical analysis was carried out using R version 2.15.2 (http://www.R-project.org/). The oligoclonality index (OCI; Gini coefficient)[6,21] was calculated using the R reldist package[22] (http://CRAN.R-project.org/package=reldist). Two-tailed nonparametric tests (Mann Whitney *U*, Fisher's exact, χ^2) were used for all comparisons. Bonferroni's correction for multiple testing was applied where appropriate. To test the hypothesis that 2 observed HTLV-1 integration sites were present in 1 T-cell clone, we used the Gaussian approximation to the binomial distribution (supplemental Figure 3). To identify clusters of integration sites or genomic hotspots of integration, we used R software developed by Presson et al[23] (http://www.biomedcentral.com/1471-2105/12/367). Functional categories of genes were analyzed through the use of Ingenuity Pathway Analysis (Ingenuity Systems; http://www.ingenuity.com).

Results

The ATL samples are derived from a representative cohort

We analyzed 197 cases of ATL; patients' characteristics are detailed in supplemental Figure 4. Systematic analysis of the proviral structure showed a complete provirus in 46% of cases, putatively capable of Tax expression; 39% of cases contained a defective provirus, 7% contained a nonsense mutation of the *tax* gene, and 8% contained a hypermethylated promoter in the 5′ LTR. There was no significant difference in OCI between ATL clinical subtypes (median OCI = 0.91) or by proviral subtype (median OCI = 0.91); the median OCI in asymptomatic carriers was 0.33, in the range previously reported[6] (Figure 1).

The median absolute number of HTLV-1^+ T-cell clones (estimated by the DivE technique) in the circulation in ACs was 9054. The median number of clones in the ATL cases was 1741 (assuming PBMC = 3×10^9/L) or 2154 (assuming PBMC = 50×10^9/L). These results show that although the white cell count may vary over an order of magnitude between individuals with ATL, the estimated number of distinct clones underlying the malignant clone remains relatively stable (~2000).

In 91% of ATL cases, a single copy of HTLV-1 is integrated into the host genome

In our protocol, the quasi-random DNA shearing by sonication allows unbiased, quantitative detection of proviruses[6,24] and therefore

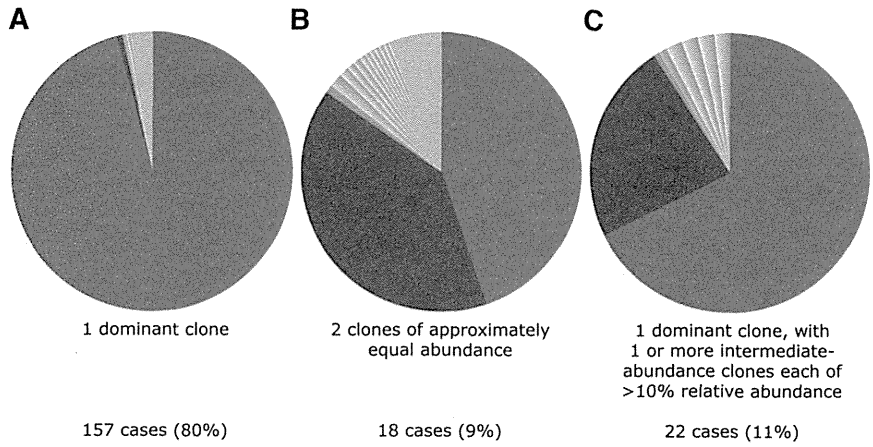

Figure 2. Examples of 3 typical clonal structures of ATL cases. Each sector in the pie charts depicts the relative abundance of the respective integration site. (A) Typical "monoclonal" ATL tumor sample; PVL = 63% (*relative abundance of dominant clone* = 97% of PVL). (B) Two equally abundant integration sites (relative abundance respectively 44% and 39% of PVL); PVL = 9%. (C) ATL with dominant clone and additional intermediate-abundance clone (relative abundance respectively 67% and 23% of PVL); PVL = 241%.

enabled us to quantify the presence of 2 abundant integration sites in an ATL tumor (Figure 2). In 157 out of 197 samples (80%), as expected, a single dominant proviral integration site was observed, with a median relative abundance of 99.4% of the PVL (range, 35% to 100%). However, in 40 out of 197 samples (20%), the presence of only a single provirus was less certain, because >1 abundant integration site was observed. In each of these 40 cases, there was 1 "large" ATL integration site with relative abundance >35% and an additional site with a relative abundance >10%. The question arises whether these represented 2 proviruses in 1 malignant clone or if there were 2 distinct abnormally expanded clones. If a single malignant clone contains 2 proviruses, then each will be present at the same frequency, assuming a steady kinetic state and no recent reinfection with a second provirus, and the clone will carry a single TCR gene rearrangement. Alternatively, if there are 2 large independent clones, then the 2 integration sites will differ in abundance and 2 distinct TCR gene rearrangements will be detected. We found no significant difference in the abundance of 2 integration sites in 18 cases (9.1% of cohort) (supplemental Figure 3), suggesting the presence of 2 proviruses in a single tumor clone. In 22 cases (11% of the cohort), we observed a large ATL clone and a second clone of abnormal but significantly lower abundance. TCR-γ gene rearrangement analysis of these 40 samples confirmed a monoclonal population in 7 out of 40 cases (3.1%); this technique may underestimate monoclonality, owing to the possibility of a second rearranged TCR-γ allele. To conclude, a single dominant provirus was detected in 91% of cases, whereas in 9% of tumors there was evidence of 2 proviruses. These results are consistent with the finding of multiple proviruses in 11% of cases reported by Tamiya et al[16] using low-throughput techniques.

Binning of clones into small, intermediate, or large

In subsequent analysis, each clone was binned according to its relative abundance, ie, the proportion of the subject's PVL occupied by that clone. Each ATL case contained at least 1 abundant clone with a relative abundance >35% (n = 217 clones) that was defined as large; "small" clones were defined as those of relative abundance <1% (n = 5925), and such clones constitute the great bulk of PVL in nonmalignant HTLV-1 infection.[6,13] Clones (n = 90) that constituted between 1% and 35% of PVL were classified as intermediate abundance. Clones (n = 16 909) identified in the AC cohort were analyzed together, because only 4 of these clones fulfilled the large-clone classification (supplemental Figure 2).

Large ATL clones have the same genomic characteristics as small (nonmalignant) clones, whereas intermediate-sized clones have unique genomic characteristics

The intermediate-abundance clones observed in 24% of cases (48/197) in addition to the large (presumed malignant) clone were larger (ie, had a greater absolute abundance) than any clones previously observed in AC or HAM/tropical spastic paraparesis cohorts.[6,13] Because progressive oligoclonal proliferation has been postulated to precede malignant transformation, we tested the hypothesis that there is a stepwise progression in the frequency of integration site characteristics from low-abundance clones through intermediate-abundance to large ATL clones. The results showed that the large, presumed malignant ATL clones had integration site characteristics indistinguishable from those of the low-abundance clones present in ACs and in patients with ATL. In contrast, the integration sites present in the intermediate-abundance clones in ATL patients, which are not observed in nonmalignant infection, differed from both the low- and high-abundance clones in each genomic attribute examined (Figure 3). Specifically, the intermediate-abundance clones lacked the associations observed in the ACs and in the low-abundance and high-abundance clones seen in ATL, with either transcriptional orientation or proximity to transcription start sites, cytosine guanine dinucleotide islands, or activatory epigenetic marks. Instead, the intermediate-abundance clones showed an association with proximity to inhibitory epigenetic marks (Figure 3C) and specific transcription-factor binding sites (TFBSs) within 100 bp upstream or downstream of the integration site, notably binding sites for P300/CBP-associated factor (odds ratio [OR] = 4.78), Rad 21 (part of the cohesin complex) (OR = 4.08), and ZNF263 (OR = 5.57). These effects disappeared at 1 kb from the integration site (Figure 3A). Integration in proximity to these specific TFBSs was identified in 8 out of 197 tumor samples (4.1% of cohort).

There are no hotspots of integration associated with large ATL clones

All data sets were further annotated to investigate the proximity of the integrated provirus to the nearest cancer-associated gene. The frequency of integration was significantly higher than random expectation within 10 kb of oncogenes in clones from ACs and low-abundance clones from ATL patients, and within 150 kb in the large ATL clones; this association was not observed in the intermediate-abundance clones. We conclude that integration in proximity to these cancer-related genes confers a survival advantage

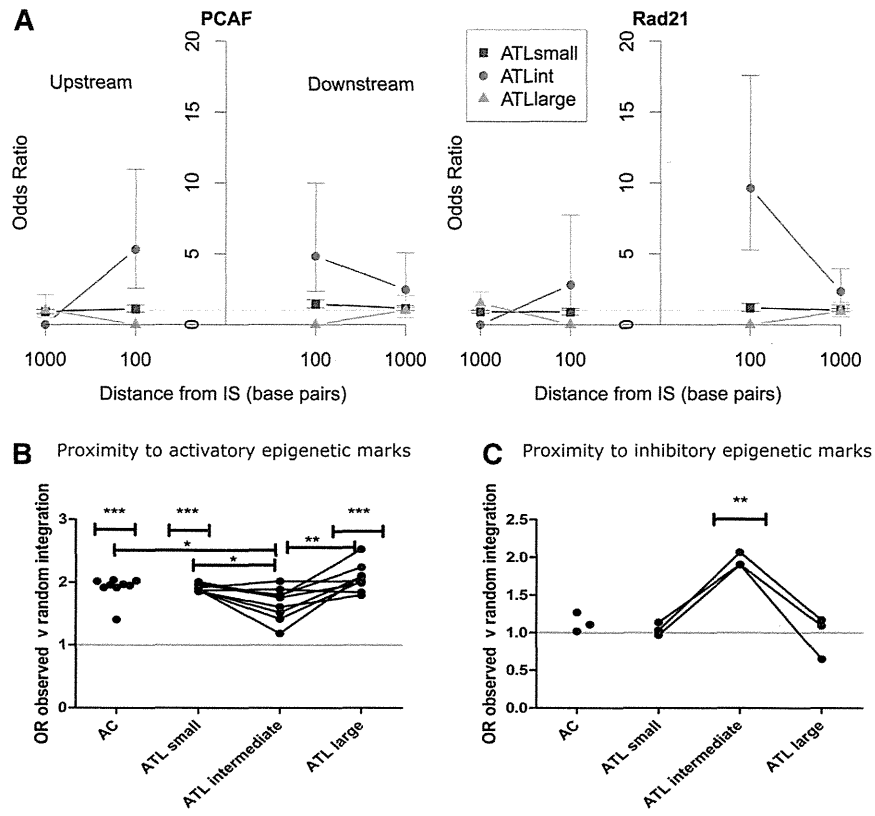

Figure 3. Intermediate-abundance clones in ATL cases contained proviruses with distinct genomic marks. (A) The OR of integration in proximity to specific TFBSs compared with AC is illustrated for 2 TFBSs, P300/CBP-associated factor binding sites (PCAFbsites) and Rad21. (See supplemental Figure 1 for full list of TFBSs tested). The y-axis shows the OR compared with ACs. The x-axis shows the distance in base pairs (logarithmic scale) from the integration site upstream (left-hand side) or downstream (right-hand side). "Upstream" and "downstream" are defined with respect to the sense strand of the HTLV-1 provirus. The junction of the x-axis and y-axis represents the integration site. There were no independent TFBS predictors for small clones (blue squares) or large clones (green triangles) in ATL cases compared with ACs (OR = 1) or when compared with each other or to random data sets (not illustrated). Independent TFBSs associated with intermediate-abundance clones in ATL cases (red circles) (PCAFbsites, Rad21) at 100 bp upstream or downstream compared with ACs are illustrated. (B) OR of integration in proximity to activatory epigenetic marks compared with random sites. AC, small, and large clones in ATL cases showed a significant bias toward integration in proximity to activatory epigenetic marks. There was no such bias in the intermediate-abundance clones. (C) OR of integration in proximity to inhibitory epigenetic marks compared with random. AC, small, and large clones in ATL cases showed no bias toward integration in proximity to inhibitory marks compared with random sites, whereas intermediate-abundance clones showed a bias toward inhibitory epigenetic marks (see supplemental Figure 1 for details of epigenetic marks tested). IS, integration site.

in vivo but does not play a significant role in leukemogenesis per se. The use of the powerful bioinformatic method of Presson et al[23] confirmed that there were no significant hotspots of integration associated with ATL.

The ontology of the nearest downstream gene was associated with the malignant clone in 6% of ATL cases

As a further test of the hypothesis that HTLV-1 proviral integration near host genes in a certain functional category confers a proliferative advantage on the infected T-cell clone, we used Ingenuity Pathway Analysis software to analyze the ontology of the nearest host genes upstream and downstream of each integration site. The results showed a significant overrepresentation of genes in 3 cellular pathways ("cell morphology," "immune cell trafficking," and "hematological system development and function") in the large ATL ("malignant") clones, but not in either the low- or intermediate-abundance clones (Figure 4). The 11 genes responsible for this significant association (*CD46*, *ITGA4*, *DPYSL2*, *RAP2A*, *CASP8*, *CDKN2A*, *GTF2I*, *TACR1*, *BCL2*, *IL6ST*, and *HGF*) accounted for 11 ATL cases (5.8% of the cohort) of different clinical subtypes. Furthermore, these effects were only seen in the nearest host gene downstream, regardless of its transcriptional orientation relative to the provirus. The median distance from the integration site to these nearest genes was 13.7 kb (range, 0.6-294 kb) compared with a median distance of 122.3 kb from all integration sites to the nearest cancer-associated gene (P = .009, Mann Whitney U test).

The HTLV-1 provirus preferentially survives in acrocentric chromosomes in vivo

Meekings et al[25] reported that the frequency of HTLV-1 proviruses in chromosome 13 was significantly higher in vivo than expected by chance, but the biological significance of this observation was uncertain. Here, using our quantitative, high-throughput technique, we observed a significant excess of integrations in chromosomes 13, 14, 15, and 21 compared with random and in vitro data sets. This excess was seen in all infected individuals and was not confined to those with ATL. There was a trend toward excess integrations in chromosome 22, but this was not statistically significant (Figure 5). These findings were validated with a second cohort of independent AC samples from the Kagoshima region of Japan. The chromosomal distribution of proviruses in the intermediate-abundance and large ATL clones was not significantly different from random, perhaps because of the small number of clones (n = 307).

Discussion

Oligoclonal proliferation of HTLV-1–infected T-cells is a cardinal feature of HTLV-1 infection. It has long been believed that this oligoclonal proliferation is primarily responsible for maintaining the high PVL of HTLV-1, which is the strongest correlate of risk of both the inflammatory (HAM) and malignant (ATL) diseases. However, we recently showed that the PVL correlates with the total number of infected clones, but not with the degree of oligoclonal proliferation as measured by the OCI.[6,13] Here, we show that ATL is frequently accompanied by a population of abnormally abundant HTLV-1–infected T-cell clones underlying the largest, putatively malignant clone. This observation suggested that such intermediate-abundance clones might represent an intermediate stage of malignant transformation between the low-abundance clones and the fully transformed, largest clone. However, we found that the host genomic attributes of the integration site in the large ATL clones closely

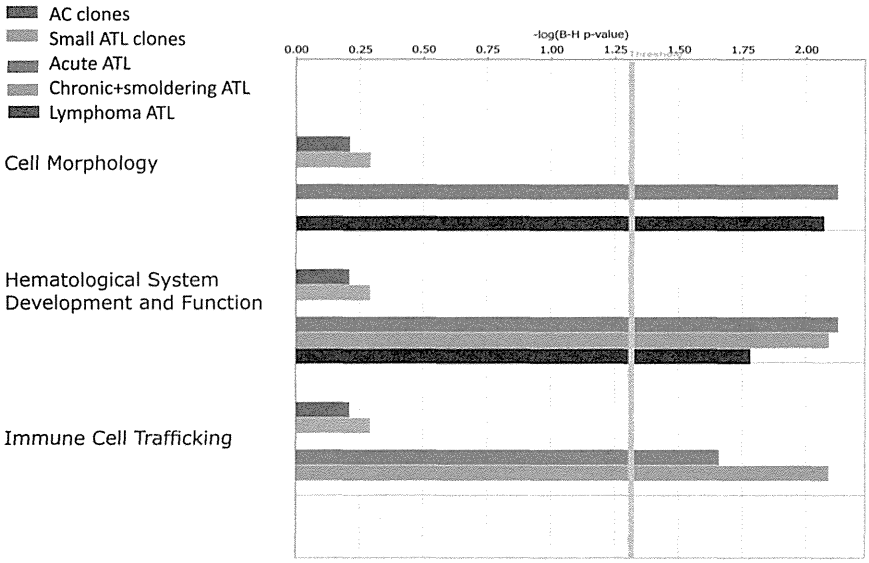

Figure 4. Functional classification of gene ontologies overrepresented among the large ATL clones. Functional categories significantly overrepresented among the random, AC, ATL small, intermediate, and large ATL clones as analyzed by Ingenuity software using the Ingenuity Pathways Knowledge Base (IPKB) gene population as baseline. Horizontal bars are only visible where there was a statistical overrepresentation of the pathway compared with the IPKB. Because there were no overrepresented pathways involving the random integration sites or intermediate-abundance clones in ATL cases, the bars are not visible. The vertical yellow threshold represents the line of statistical significance ($P < .05$) after correction (Benjamini-Hochberg) for multiple testing. The numbers of searchable genes for comparison with the IPKB were random (n = 96 706), AC (n = 5679), ATL small (n = 1628), ATL intermediate (n = 87), or ATL large (acute n = 141, lymphoma n = 31, chronic and smoldering n = 38).

resembled those of the low-abundance clones present both in ATL patients and in those with nonmalignant infection, whereas the integration site characteristics of the intermediate-abundance clones differed from both the low- and high-abundance clones and from the clones observed in nonmalignant cases of HTLV-1 infection. We conclude that the malignant clone does not arise from the intermediate-abundance clones but instead from the low-abundance clones. This conclusion is consistent with the observations that the low-abundance clones constitute the bulk of the PVL in HTLV-1 infection[6] and that the risk of ATL is correlated with the PVL.[2,4] We have also observed cases in which the malignant clone emerges from the large population of low-abundance clones, not from the preexisting oligoclonally expanded population.[26] Finally, this conclusion is also consistent with our recent observation[27] of highly oligoclonal proliferation and a small total number of clones in human T-lymphotropic virus type 2 infection, which does not cause malignant disease.

We therefore propose that the major determinant of the risk of ATL is the absolute number of clones: the larger the number, the greater the chance of malignant transformation. It is likely that the number of HTLV-1–infected clones present in an individual during chronic infection is determined chiefly by the efficiency of the host's CTL response to the virus, which in turn is determined by the HLA and killer immunoglobulin-like receptor genotype.[10,28]

The observation that the abnormally expanded intermediate-abundance clones seen in patients with ATL do not share genomic characteristics with either the polyclonal background or the malignant clones suggests that the intermediate-abundance clones arise as a consequence of ATL development and are not causative. One possibility is that these clones survive and proliferate as a consequence of the severely impaired immune response in ATL. The malignant clones in ATL use well-described mechanisms to silence Tax, either before or after malignant transformation, which allows them to escape the immunodominant CTL response and so confers a survival advantage. Once the malignant clone has emerged, the resulting immune impairment may allow the intermediate-abundance clones to survive despite continued expression of viral genes.

As expected, we did not identify any hotspots of integration, although analysis of the ontology of flanking genes demonstrated a functional overrepresentation of certain genes that are known to be dysregulated in many leukemias. This effect was significant only in the large (presumed malignant) ATL clones and only when considering the ontology of the nearest host gene downstream; there was no effect of the upstream host gene. Further, these specific genes lay very close (median 13.7 kb) to the provirus, suggesting a mechanistic interaction between the provirus and the downstream gene. Although the associations reported here between ATL and individual genes and genomic features account for a small proportion of the observed cases of ATL, these results indicate that transcriptional interactions between the provirus and the flanking host genome influence the risk of malignant transformation. Vogelstein recently estimated that each tumor-driver mutation contributes a survival advantage of ~0.4% to

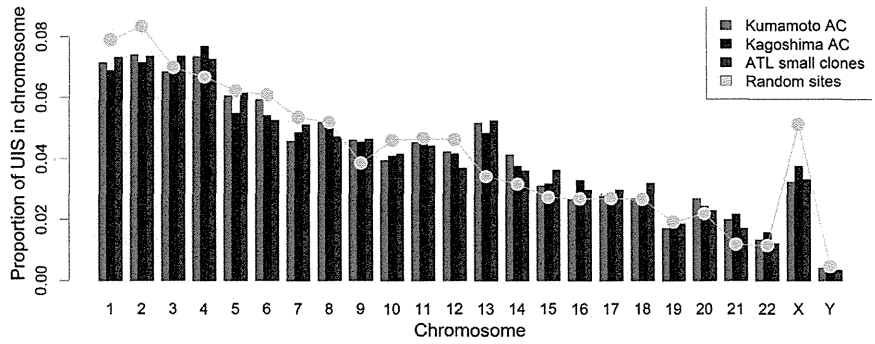

Figure 5. Preferential survival of HTLV-1 in vivo in chromosomes 13, 14, 15, and 21. The proportion of unique integration sites (UIS) per chromosome is shown for 2 independent AC data sets (Kumamoto and Kagoshima) and the small clones in ATL cases. The yellow line shows the frequency of sites in the random data set. There were an increased number of integrations in chromosomes 13, 14, 15, and 21 in the clones of asymptomatic carriers and small clones in ATL cases compared with random. The bias remained in chromosomes 13 and 15 when compared with a previously reported data set[6] of integration sites from Jurkat cells infected in vitro with HTLV-1.

a clone[29]; the HTLV-1 genomic integration site may contribute a similar advantage.[26]

A further unexpected observation was the preferential survival in vivo of the HTLV-1 provirus in the acrocentric chromosomes 13, 14, 15, 21, and (although not reaching formal significance) 22. Throughout most of the cell cycle, these chromosomes are physically associated with the nucleolus, and they encode the machinery of the ribosome on the short (p) arm. Because the HTLV-1 proviral integration sites are found only in the long (q) arm of these chromosomes, we postulate that the selective advantage enjoyed by these clones derives not from the proviral integration near the ribosome-coding genes but rather from the physical location of the provirus-containing chromatin in the nucleus, perhaps by coupling proviral transcription to transcription of the acrocentric chromosomes. Experiments are underway to test this hypothesis.

Acknowledgments

The authors thank Nirav Malani and Frederic D. Bushman at the department of Microbiology, University of Pennsylvania, Philadelphia, PA for the list of random integration sites and for developing software packages and the Core Genomics Laboratory at the MRC Clinical Sciences Centre, Hammersmith Hospital, London, United Kingdom. The authors thank Aileen Rowan and Yorifumi Satou for many helpful discussion and comments and the patient donors in Japan.

This work was funded by Leukaemia and Lymphoma Research and the Wellcome Trust.

Authorship

Contribution: L.B.C., G.P.T., M.M., and C.R.M.B. conceived and designed the experiments; M.M. performed the clinical diagnosis; L.B.C. performed the experiments; M.V. and L.F. performed and interpreted TCR studies; L.B.C. analyzed the data; A.M., H.N., and D.J.L. contributed to the bioinformatic and statistical analysis, tools, and data sets; and L.B.C. and C.R.M.B. wrote the paper.

Conflict-of-interest disclosure: The authors declare no competing financial interests.

Correspondence: Charles R. M. Bangham, Wright-Fleming Institute, Imperial College, Norfolk Place, London, W2 1PG, United Kingdom; e-mail: c.bangham@imperial.ac.uk.

References

1. Shimoyama M. Diagnostic criteria and classification of clinical subtypes of adult T-cell leukaemia-lymphoma. A report from the Lymphoma Study Group (1984-87). *Br J Haematol.* 1991;79(3):428-437.
2. Sasaki D, Doi Y, Hasegawa H, et al. High human T cell leukemia virus type-1(HTLV-1) provirus load in patients with HTLV-1 carriers complicated with HTLV-1-unrelated disorders. *Virol J.* 2010;7:81.
3. Iwanaga M, Watanabe T, Utsunomiya A, et al; Joint Study on Predisposing Factors of ATL Development investigators. Human T-cell leukemia virus type I (HTLV-1) proviral load and disease progression in asymptomatic HTLV-1 carriers: a nationwide prospective study in Japan. *Blood.* 2010;116(8):1211-1219.
4. Demontis MA, Hilburn S, Taylor GP. Human T cell lymphotropic virus type 1 viral load variability and long-term trends in asymptomatic carriers and in patients with human T cell lymphotropic virus type 1-related diseases. *AIDS Res Hum Retroviruses.* 2013;29(2):359-364.
5. Overbaugh J, Bangham CR. Selection forces and constraints on retroviral sequence variation. *Science.* 2001;292(5519):1106-1109.
6. Gillet NA, Malani N, Melamed A, et al. The host genomic environment of the provirus determines the abundance of HTLV-1-infected T-cell clones. *Blood.* 2011;117(11):3113-3122.
7. Cook LB, Rowan AG, Melamed A, Taylor GP, Bangham CR. HTLV-1-infected T cells contain a single integrated provirus in natural infection. *Blood.* 2012;120(17):3488-3490.
8. Tsukasaki K, Tsushima H, Yamamura M, et al. Integration patterns of HTLV-I provirus in relation to the clinical course of ATL: frequent clonal change at crisis from indolent disease. *Blood.* 1997;89(3):948-956.
9. Matsuoka M, Jeang KT. Human T-cell leukemia virus type 1 (HTLV-1) and leukemic transformation: viral infectivity, Tax, HBZ and therapy. *Oncogene.* 2011;30(12):1379-1389.
10. Bangham CR. CTL quality and the control of human retroviral infections. *Eur J Immunol.* 2009; 39(7):1700-1712.
11. Nagai M, Usuku K, Matsumoto W, et al. Analysis of HTLV-I proviral load in 202 HAM/TSP patients and 243 asymptomatic HTLV-I carriers: high proviral load strongly predisposes to HAM/TSP. *J Neurovirol.* 1998;4(6):586-593.
12. Jeffery KJ, Usuku K, Hall SE, et al. HLA alleles determine human T-lymphotropic virus-I (HTLV-I) proviral load and the risk of HTLV-I-associated myelopathy. *Proc Natl Acad Sci USA.* 1999;96(7): 3848-3853.
13. Melamed A, Laydon DJ, Gillet NA, Tanaka Y, Taylor GP, Bangham CR. Genome-wide determinants of proviral targeting, clonal abundance and expression in natural HTLV-1 infection. *PLoS Pathog.* 2013;9(3):e1003271.
14. Nosaka K, Maeda M, Tamiya S, Sakai T, Mitsuya H, Matsuoka M. Increasing methylation of the CDKN2A gene is associated with the progression of adult T-cell leukemia. *Cancer Res.* 2000;60(4): 1043-1048.
15. Kwok S, Ehrlich G, Poiesz B, Kalish R, Sninsky JJ. Enzymatic amplification of HTLV-I viral sequences from peripheral blood mononuclear cells and infected tissues. *Blood.* 1988;72(4): 1117-1123.
16. Tamiya S, Matsuoka M, Etoh K, et al. Two types of defective human T-lymphotropic virus type I provirus in adult T-cell leukemia. *Blood.* 1996; 88(8):3065-3073.
17. Takeda S, Maeda M, Morikawa S, et al. Genetic and epigenetic inactivation of tax gene in adult T-cell leukemia cells. *Int J Cancer.* 2004;109(4): 559-567.
18. Barski A, Cuddapah S, Cui K, et al. High-resolution profiling of histone methylations in the human genome. *Cell.* 2007;129(4):823-837.
19. Sadelain M, Papapetrou EP, Bushman FD. Safe harbours for the integration of new DNA in the human genome. *Nat Rev Cancer.* 2012;12(1): 51-58.
20. Laydon DJ, Melamed A, Sim A, et al. Quantification of HTLV-1 clonality and TCR diversity. *PLOS Comput Biol.* In press.
21. Gini C. Variabilita e Mutuabilita. Contributo allo Studio delle Distribuzioni e delle Relazioni Statistiche. Bologna, Italy: C. Cuppini; 1912.
22. Handcock M, Morris M. Relative Distribution Methods in the Social Sciences. New York, NY: Springer-Verlag; 1999.
23. Presson AP, Kim N, Xiaofei Y, Chen IS, Kim S. Methodology and software to detect viral integration site hot-spots. *BMC Bioinformatics.* 2011;12:367.
24. Berry CC, Gillet NA, Melamed A, Gormley N, Bangham CR, Bushman FD. Estimating abundances of retroviral insertion sites from DNA fragment length data. *Bioinformatics.* 2012;28(6): 755-762.
25. Meekings KN, Leipzig J, Bushman FD, Taylor GP, Bangham CR. HTLV-1 integration into transcriptionally active genomic regions is associated with proviral expression and with HAM/TSP. *PLoS Pathog.* 2008;4(3):e1000027.
26. Bangham CRM, Cook LB, Melamed A. HTLV-1 clonality in adult T-cell leukaemia and non-malignant HTLV-1 infection [published online ahead of print December 6, 2013]. *Semin Cancer Biol.*
27. Melamed A, Witkover AD, Laydon DJ, et al. Clonality of HTLV-2 in natural infection. *PLoS Pathog.* 2014;10(3):e1004006.
28. Macnamara A, Rowan A, Hilburn S, et al. HLA class I binding of HBZ determines outcome in HTLV-1 infection. *PLoS Pathog.* 2010;6(9): e1001117.
29. Vogelstein B, Papadopoulos N, Velculescu VE, Zhou S, Diaz LA Jr, Kinzler KW. Cancer genome landscapes. *Science.* 2013;339(6127): 1546-1558.

blood

2014 123: 3925-3931
doi:10.1182/blood-2014-02-553602 originally published online April 15, 2014

The role of HTLV-1 clonality, proviral structure, and genomic integration site in adult T-cell leukemia/lymphoma

Lucy B. Cook, Anat Melamed, Heather Niederer, Mikel Valganon, Daniel Laydon, Letizia Foroni, Graham P. Taylor, Masao Matsuoka and Charles R. M. Bangham

Blood (print ISSN 0006-4971, online ISSN 1528-0020), is published weekly by the American Society of Hematology, 2021 L St, NW, Suite 900, Washington DC 20036.

Reevaluation of confirmatory tests for human T-cell leukemia virus Type 1 using a luciferase immunoprecipitation system in blood donors

Rika A. Furuta,[1] Guangyong Ma,[2] Masao Matsuoka,[2] Satoshi Otani,[1] Harumichi Matsukura,[1] and Fumiya Hirayama[1]

BACKGROUND: Recently, Japanese Red Cross blood centers have changed the confirmatory test method from an indirect immunofluorescence (IF) technique to Western blotting (WB) for antibodies against human T-cell leukemia virus Type 1 (HTLV-1). In this study, these HTLV-1 tests were assessed using another sensitive method, that is, a luciferase immunoprecipitation system (LIPS), to identify a better confirmatory test for HTLV-1 infection.

STUDY DESIGN AND METHODS: Plasma samples from 54 qualified donors and 114 HTLV-1 screening–positive donors were tested by LIPS for antibodies against HTLV-1 Gag, Tax, Env, and HBZ recombinant proteins. The donors were categorized into six groups, namely, (Group I) qualified donors, screening positive; (Group II) IF positive; (Group III) IF negative; (Group IV) WB positive; (Group V) WB negative; and (Group VI) screening positive in the previous blood donation, but WB-indeterminate during this study period.

RESULTS: In Groups II and IV, all plasma samples tested positive by LIPS for antibodies against Gag and Env proteins. In Group V, all samples tested negative by LIPS, whereas some Group III samples reacted with single or double antigens in LIPS. In Group VI, the LIPS test identified a donor with suspected HTLV-1 infection. The first case of a blood donor with plasma that reacted with HBZ was identified by LIPS.

CONCLUSION: Reevaluation of the current HTLV-1 screening method using the LIPS test showed that both confirmatory tests had similar sensitivity and specificity only when WB indeterminate results were eliminated. LIPS is a promising method for detecting and characterizing HTLV-1 antibodies.

On September 19, 2012, Japanese Red Cross (JRC) blood centers changed the confirmatory test method for blood donors testing positive for human T-cell leukemia virus Type 1 (HTLV-1) antibodies during screening using an automated chemiluminescence enzyme-linked immunoassay (CLEIA) test (CL4800 testing system, Fujirebio, Shinjuku Ward, Tokyo, Japan) from an in-house cell-based indirect immunofluorescence technique (IF) test[1] to a commercial Western blotting (WB) test (ProBlot HTLV-1, Fujirebio) to reduce the number of false-positive results. In our donor screening method, all blood samples were disqualified if they were collected from donors who tested positive in CLEIA screening tests for transfusion-transmitted infections, including hepatitis B and C viruses, human immunodeficiency virus Types 1 (HIV-1) and 2 (HIV-2), HTLV-1, *Treponema pallidum*, and parvovirus B19. These screening tests were established with high sensitivities while

ABBREVIATIONS: ATL = adult T-cell leukemia; CLEIA = chemiluminescence enzyme-linked immunoassay; HAM/TSP = HTLV-1–associated myelopathy/tropical spastic paraparesis; IF = indirect immunofluorescence; JRC = Japanese Red Cross; LIPS = luciferase immunoprecipitation system; RLU(s) = relative luciferase unit(s); WB = Western blotting.

From the [1]Japanese Red Cross, Kinki Block Blood Center, Osaka, Japan; and the [2]Laboratory of Virus Control, Institute for Virus Research, Kyoto University, Kyoto, Japan.

Address reprint requests to: Rika A. Furuta, 7-5-17 Saito-Asagi, Ibaragi City, Osaka 567-0085, Japan; e-mail: r-furuta@kk.bbc.jrc.or.jp.

Supported by Blood Service Headquarters, Japanese Red Cross Society.

Received for publication May 14, 2014; revision received August 21, 2014, and accepted September 6, 2014.

doi: 10.1111/trf.12911

TRANSFUSION 2015;55:880–889.

sacrificing their specificities to ensure the safety of transfusion medicine, yielding a substantial amount of false-positive results. A confirmatory test for HTLV-1 was implemented to identify infected donors, who were notified about their test result if they wished. However, the WB test for HTLV-1 still occasionally produced unclear results, represented as WB indeterminate.[2]

The luciferase immunoprecipitation system (LIPS) is an antibody detection method with high sensitivity, which uses recombinant antigens fused with the luciferase protein. The amount of luciferase-fused antigen captured by antibodies in a test sample is measured as the luciferase activity without using secondary antibodies for detection. LIPS was originally developed to analyze whole proteome antibody response profiles,[3] but it was subsequently applied to the detection of anti-HTLV in asymptomatic carriers and patients with adult T-cell leukemia (ATL) or HTLV-1–associated myelopathy/tropical spastic paraparesis (HAM/TSP).[4] In the latter study, all HTLV-1–infected subjects, including 15 asymptomatic carriers, tested positive for antibodies against the Gag protein by LIPS, while 62 of 73 and 71 of 73 tested positive for antibodies against Env or Tax proteins, respectively. These results suggested that the LIPS test for Gag antibodies would exclude donors with false-positive or WB-indeterminate results in our HTLV-1 confirmatory tests. Therefore, we constructed a series of plasmids that encoded the genes for HTLV-1 Gag, Tax, Env, or HBZ fused with *Renilla* luciferase (Promega, Madison, WI) and reevaluated the positive plasma samples collected during the screening period immediately before and after changing the confirmatory test method. We analyzed 114 HTLV-1 screening–positive plasma samples and 54 screening-negative plasma samples by LIPS for antibodies against four viral antigens to determine the quality of our confirmatory test for HTLV-1 and explore the potential utility of HTLV-1 LIPS tests for blood donors.

MATERIALS AND METHODS

Test subjects

In JRC blood centers, the routine tests applied to detect transfusion-transmitted infections are performed using donor sera. This study used plasma that was stored at –40°C in all the LIPS tests. Plasma samples that tested positive for HTLV-1 antibodies in the screening tests were collected between August 1 and October 23, 2012. In addition, 54 plasma samples were collected from qualified donors as negative controls (categorized as Group I). Among the screening-positive plasma samples, 17 tested positive by IF (Group II), 36 tested negative by IF (Group III), 21 tested positive by WB (Group IV), and 14 tested negative by WB (Group V). Group VI comprised 26 plasma samples collected from donors who tested positive by CLEIA during the previous blood donation and showed indeterminate test results by WB during the study period. Thirteen of the 26 plasma samples in Group VI tested positive and the remaining were negative by CLEIA at the time of donation during the study period. The identifiers used for the positive plasma samples in Group VI were VI-1, -3, -5, -6, -9, -10, -12, -15, -18, -22, -24, -25, and -26. In addition, plasma samples from Groups II and III were examined by WB and those from Groups IV to VI were examined by IF. All the plasma samples were analyzed after receiving informed consent from the corresponding donors during blood donation.

Expression vectors for HTLV-1 LIPS antigens

To express HTLV-1 antigens fused with *Renilla* luciferase, we eliminated the codon of the first methionine in *Renilla* luciferase in the pGL4.75 plasmid (Promega) via site-directed mutagenesis. A synthetic cDNA fragment of the HTLV-1 Gag precursor, Env precursor, Tax, or HBZ, from which the stop codons were eliminated, was then inserted at the N-terminus of the mutated *Renilla* luciferase plasmid (pGL4.75ΔMet) with the spacer amino acids "Gly-Gly-Arg-Gly," thereby generating the plasmids designated as pGagRLuc, pTaxRLuc, pEnvRLuc, and pHBZRLuc, respectively. To produce an additional HBZ protein, which was fused with *Renilla* luciferase in the opposite order to that of pHBZRLuc, we also mutagenized the pGL4.75 plasmid to eliminate a stop codon in *Renilla* luciferase cDNA and replaced it with a new Asp718 enzyme recognition sequence, thereby generating the pGL4.75Asp718 plasmid. The HBZ cDNA was amplified by PCR using a forward primer containing the Asp718 recognition sequences and a reverse primer containing the *Xba*I recognition sequence, which was originally located at the end of the *Renilla* luciferase cDNA. The resultant plasmid, pRLucHBZ, expressed *Renilla* luciferase fused with the HBZ protein at the C-terminus with Gly-Gly-Thr spacer amino acids. The GenBank accession numbers of the HTLV-1 sequences used in this study are NC_001436 for Gag, Env, and Tax and DQ273132 for HBZ. The oligonucleotide sequences used for site-directed mutagenesis were as follows: 5′-gaattcgcactcgagtggcttccaaggtgtacg-3′ and 5′-gagctcacgcttaagaccaccgaaatggttgtc-3′ for pGL4.75ΔMet and 5′-cagggaggtaccttctagagtcggggcggc-3′ and 5′-gaaggtacctccctgctcgttcttcagcac-3′ for pGL4.75Asp718. The sequences of the PCR primers used to amplify HBZ cDNA with an Asp718 enzyme recognition sequence were as follows: forward primer, 5′-ggtaccatggctgcaagcggactg-3′ and reverse primer, 5′-tctagattactgcagccacatagcctcca-3′.

Preparation of antigens

Human kidney 293T cells were obtained from ATCC (ATCC CRL-3216) and maintained in Dulbecco's modified Eagle's medium (Life Technologies, Carlsbad, CA), which

was supplemented with 10% fetal bovine serum and antibiotics. To transfect semiconfluent human 293T cells in a 10-cm culture dish, 12.5 μg of the *Renilla* luciferase–fused HTLV-1 antigen expression plasmid was introduced using Lipofectamine LTX (Life Technologies), according to the manufacturer's instruction. Two days after transfection, the cells were lysed with 1 mL of *Renilla* luciferase assay lysis buffer (Promega). After two cycles of freezing at −80°C and thawing at room temperature, the lysate was clarified by centrifugation at 13,000 × *g* for 5 minutes at 4°C. Aliquots of the lysate were stored at −80°C until use.

LIPS test

The LIPS tests were performed as described previously,[4] with slight modifications. In brief, 10 μL of plasma diluted 1:10 with assay Buffer A (20 mmol/L Tris, pH 7.5, 150 mmol/L NaCl, 5 mmol/L $MgCl_2$, 1% Triton X-100) was used in 100 μL of a LIPS test mixture in which 50 μL of the equivalent of 1.5×10^7 relative luciferase units (RLUs) of *Renilla* luciferase–fused antigen (293T cell lysate) and 40 μL of Buffer A were added. After being incubated for 30 minutes at room temperature, the antigen–antibody complex was captured using 7 μL of 30% protein A/G resin (Pierce, Rockford, IL) for 30 minutes at room temperature in a 96-well filter plate (MultiScreen HTS, Merck Millipore, Darmstadt, Germany). After being washed six times with Buffer A using a vacuum manifold (MultiScreen HTS, Merck Millipore), the luciferase activities were measured with a detection instrument (Glomax Multi, Promega) using 100 μL of *Renilla* luciferase assay substrate (Promega).

Immunoblotting

To determine the LIPS antigen expression levels, 1×10^6 of 293T cells were seeded 1 day before transfection and then transfected with 2.5 μg of empty pcDNA3.1(−)/myc-His (Life Technologies), or the antigen-expressing vector mentioned. Two days after transfection, the cells were lysed with 200 μL of lysis buffer (50 mmol/L Tris-Cl, pH 7.6, 150 mmol/L NaCl, 0.5% NP-40, 0.1% Na-deoxycholate, 0.1% Triton X-100). The proteins were analyzed by 5% to 20% sodium dodecyl sulfate–polyacrylamide gel electrophoresis (SDS-PAGE) and transferred onto a polyvinylidene difluoride membrane (Wako, Osaka, Japan). The recombinant LIPS antigens were detected using an anti-*Renilla* luciferase rabbit polyclonal antibody (PM047; MBL, Nagoya, Japan). To confirm the anti-HBZ in the donor plasma samples, 293T cells were transfected with 2.5 μg of pcDNA3.1(−)/myc-His, MycHis-HBZ,[5] pME-HBZ,[5] MycHis-HBZ,[5] pHBZRLuc, or pRLucHBZ using Lipofectamine LTX, according to the manufacturer's instructions. MycHis-HBZ and pME-HBZ are expression vectors for myc-6× His-tagged and wild-type HBZ proteins, respectively. SDS-PAGE and membrane transfer were performed as described above and probed with 1:500-diluted anti-HBZ rabbit polyclonal antisera[6] or 1:100-diluted donor plasma.

Statistical analysis

Computer software (IBM SPSS Statistics, Version 21.0, IBM Corp., Armonk, NY) was used for the statistical calculations. The cutoff limit for each antigen was derived from the mean value of 54 control samples plus five standard deviations (SDs), as reported previously.[4]

RESULTS

Expression of LIPS antigens

We constructed a series of plasmid vectors to express recombinant HTLV-1 antigens, which were fused with *Renilla* luciferase to detect anti-HTLV-1 by measuring the luciferase enzyme activity levels. In previous studies that used the LIPS method to detect HTLV-1 antibodies, the viral antigens were prepared as fusion proteins, where the *Renilla* luciferase protein was located at the N-terminus of each HTLV-1 protein.[4,7] We expected that the tertiary structure of the viral protein, particularly that of the envelope glycoprotein, would be less affected by the fused luciferase protein when it was placed in the opposite order because a signal sequence that mediates targeting and translocation to endoplasmic reticulum[8-10] is located at the N-terminus of the envelope glycoprotein precursor gp62. Therefore, we placed the *Renilla* luciferase protein at the C-terminus of each viral protein. Figure 1A shows the expression levels of recombinant HTLV-1 proteins fused with *Renilla* luciferase in 293T cells. First, we eliminated the codon for the first methionine of *Renilla* luciferase in the original vector (Fig. 1A, Lane 1, pGL4.75) using site-directed mutagenesis to minimize the background luciferase signals produced by intrinsic luciferase proteins in the fusion protein constructs. A small amount of the luciferase protein was detected in the mutated *Renilla* luciferase expression vector (Fig. 1A, Lane 3, pGL4.75ΔMet), which migrated slightly faster, thereby suggesting that a small amount of the luciferase protein was translated from the second (+39 bp) or third (+78 bp) codons of methionine in cDNA of *Renilla* luciferase with low efficiency. The Gag–*Renilla* luciferase and Env–*Renilla* luciferase fusion proteins were detected at the expected sizes of their precursors (Fig. 1A, Lanes 4 and 5). In our plasmids, Gag and Env proteins were expressed as the precursor Pr53 and gp62, respectively, and only small fractions of these proteins were processed in the plasmid-transfected cells. The Tax–*Renilla* luciferase and HBZ–*Renilla* luciferase fusion proteins were expressed in an efficient manner (Fig. 1A, Lanes 6 and 7). Figure 1B shows the luciferase enzyme activities (indicated as RLUs) of the

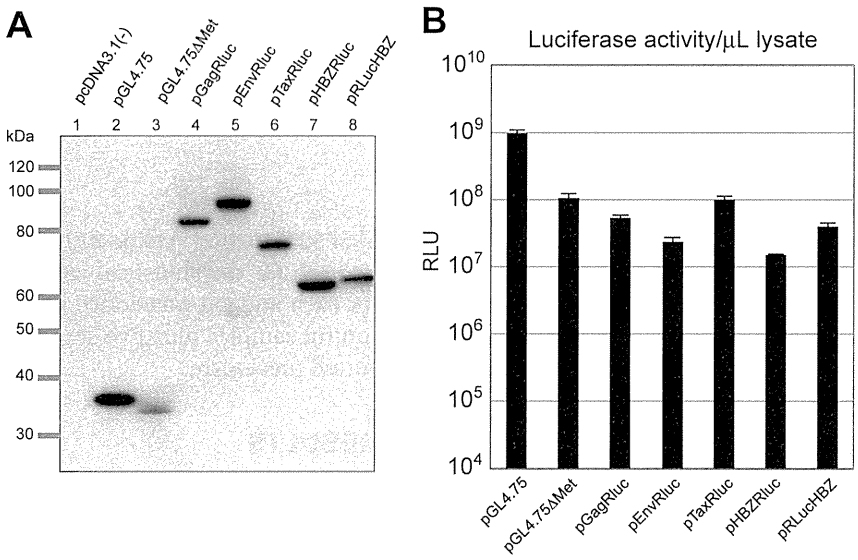

Fig. 1. Expression antigens used in HTLV-1 LIPS. Human 293T cells were transfected with each indicated plasmid, which encoded LIPS antigens, and we analyzed the protein expression levels in the cell lysates by immunoblotting with anti-*Renilla* luciferase (A) and by measuring luciferase activities (B). (A) Lanes 1-3 = pcDNA3.1(–)/myc-His, empty vector; pGL4.75, *Renilla* luciferase expression vector; pGL4.74ΔMet, pGL4.75 with a mutation in the first methionine codon. Lanes 4-8 = antigen–*Renilla* luciferase fusion protein expression vectors: Gag (Lane 4), Env (Lane 5), Tax (Lane 6), and HBZ (Lane 7). pRLucHBZ in Lane 8 = an expression vector for the *Renilla* luciferase–HBZ fusion protein. RLU, measured for 1 second.

lysates of cells transfected with each of the vectors. We also constructed a plasmid that encoded the HBZ protein fused with *Renilla* luciferase at the N-terminus of HBZ (RLucHBZ), as reported previously,[11] to examine whether the antibody responses were affected by the order of the HBZ and *Renilla* luciferase proteins. The expression level of RLucHBZ was slightly less than that of HBZRLuc (Fig. 1B, Lanes 7 and 8); however, the luciferase activity of RLucHBZ was higher than that of its counterpart (Fig. 1B).

HTLV-1 LIPS tests of blood donors

To evaluate the two types of confirmatory tests for HTLV-1, we performed the HTLV-1 LIPS test using donor plasma that had been screened by CLEIA and confirmed by IF or WB. First, we examined the reproducibility of our LIPS tests. Using one control plasma sample that tested negative for HTLV-1 by CLEIA screening and two plasma samples that tested positive by both IF and WB, we performed the LIPS test four times independently against the Gag, Env, Tax, and HBZ antigens. As shown in Fig. 2A, each LIPS result obtained from the same test subject exhibited good reproducibility in multiple tests against all four antigens, whereas the antibody responses of the same test subject varied widely between antigens. The mean of the SD was 4.9% (0.04% to 11.2% at minimum and maximum, respectively) of the mean of four test results against the same antigen. Based on these results, we performed the LIPS test once on one plasma sample in the subsequent analysis.

The luciferase activities of the individual plasma samples according to LIPS tests are shown in Fig. 2B, and the numbers of positive test results are summarized in Table 1. We categorized the donors into six groups. Group I comprised screening test–negative donor samples (negative controls). Groups II to V comprised donors who tested positive by CLEIA screening and who tested positive by IF, negative by IF, positive by WB, and negative by WB, respectively. In Group VI, the plasma collected from donors tested positive by CLEIA at the previous donation. However, indeterminate results were obtained in the WB confirmatory test during the study period; that is, the CLEIA screening results of the donors in Group VI were positive or negative during the study period. Moreover, we reexamined the plasma samples from Groups II and III by WB and those from Groups IV to VI by IF (Table 1, right-end column). As shown in Table 1, the plasma samples that tested positive in both the antibody tests, that is, screening and confirmatory tests (Groups II and IV), exhibited 100% positivity for antibodies against both Gag and Env antigens. The donors in these categories tested positive for antibodies in all three different tests, that is, CLEIA, IF or WB, and LIPS, which strongly suggests that these donors were asymptomatic carriers of HTLV-1. One plasma sample from Group II showed a weak binding to the gp46 Env antigen, as assessed in the additional WB, resulting in an indeterminate test result (Fig. 2B, asterisk). In JRC blood centers, the positive diagnosis of the HTLV-1 WB test is determined as follows: antibody responses against multiple antigens including Env gp46 and at least one antigen from Gag p19, p24, or GagPr53. Otherwise, the test results are categorized as indeterminate. In Groups II and IV, the LIPS results for the antibodies against the Gag and Env antigens indicated that both the confirmatory antibody tests had equivalent sensitivity when we excluded the results for Group VI. In Groups II and IV, we found that all the antibody responses against Env in the LIPS test were strong, whereas some plasma samples had much weaker responses against Gag. The detection results for Tax antibodies showed that more than half of the plasma samples in Groups II and IV tested positive with various intensities, as reported previously.[4,7] Among the donors who tested

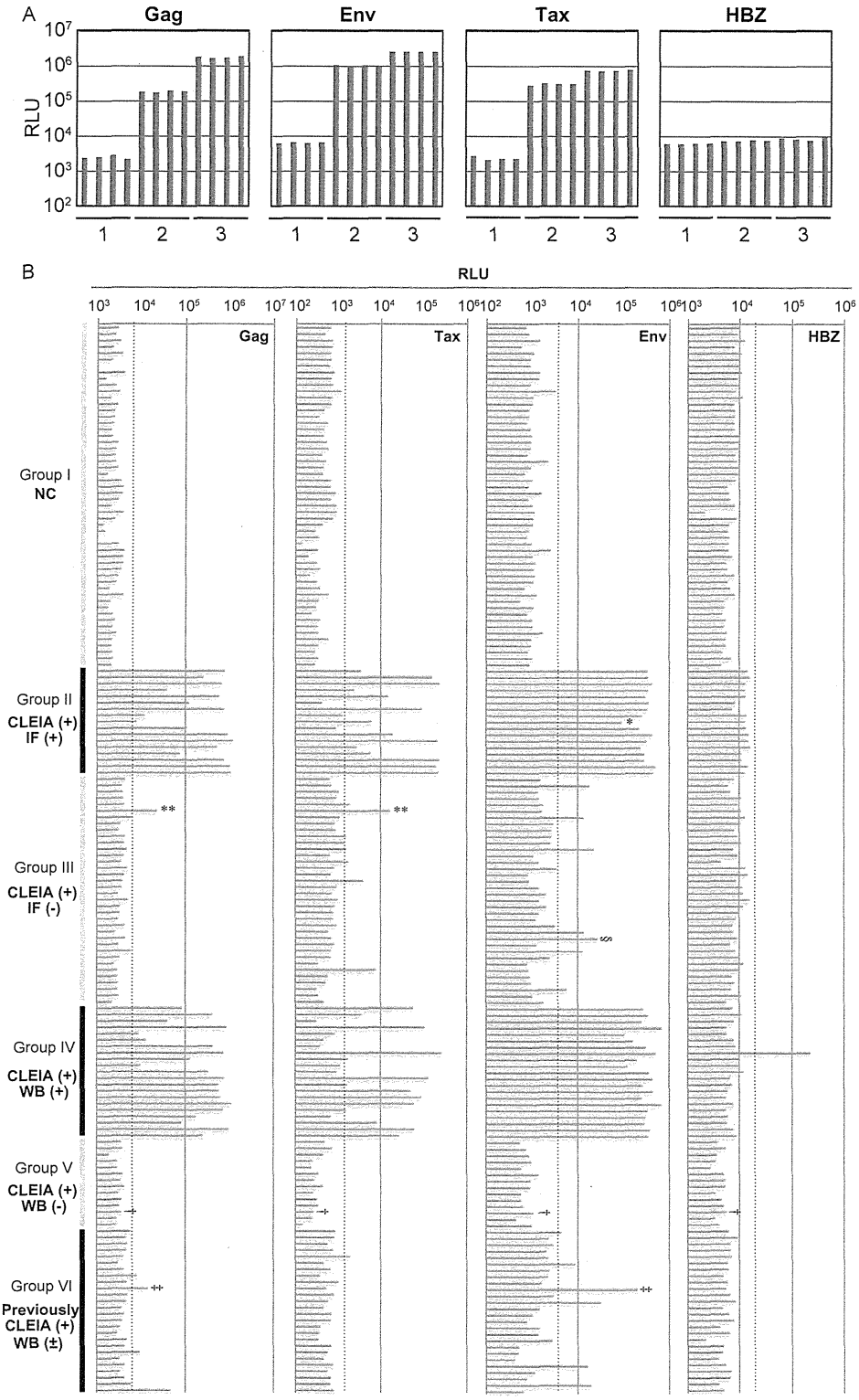

Fig. 2. Antibody responses against four viral antigens, that is, Gag, Tax, Env, and HBZ measured by LIPS. (A) HTLV-1 LIPS of representative samples. One negative control (1) and two positive control (2 and 3) plasma samples were examined by LIPS against the Gag, Env, Tax, and HBZ antigens in four independent experiments. (B) HTLV-1 LIPS of all samples. Data in the same vertical position indicate results from the same test plasma sample. Dotted lines = cutoff values (6938, 15620, 2379, and 30119 for Gag, Tax, Env, and HBZ, respectively); *plasma samples that showed a WB-indeterminate result; **plasma sample that tested positive for antibodies against Gag and Tax by LIPS; §plasma sample that tested positive by WB; †plasma sample that tested positive by IF; ‡plasma

TABLE 1. Positive results using the HTLV-1 LIPS tests

Group	Screening test (CLEIA)	Confirmatory Test 1*	Positive number/test number by LIPS (%)				Positive number/test number by Confirmatory Test 2†
			Gag	Tax	Env	HBZ	
I	Negative	ND	0/54 (0%)	0/54 (0%)	0/54 (0%)	0/54 (0%)	ND
II	Positive	Positive by IF	17/17 (100%)	14/17 (82.4%)	17/17 (100%)	0/17 (0%)	16/17 by WB (94.1%)
III	Positive	Negative by IF	1/36 (2.8%)	7/36 (19.4%)	8/36 (22.2%)	0/36 (0%)	1/36 by WB (2.8%)
IV	Positive	Positive by WB	21/21 (100%)	13/21 (61.9%)	21/21 (100%)	1/21 (4.8%)‡	21/21 by IF (100%)
V	Positive	Negative by WB	0/14 (0%)	0/14 (0%)	0/14 (0%)	0/14 (0%)	1/14 by IF (7.1%)
VI	Positive at the previous donation	WB indeterminate	4/26 (15.4%)	1/26 (3.8%)	5/26 (19.2%)	0/26 (0%)	4/26 by IF (15.4%)

* Examined through blood screening.
† Examined after the blood screening performed in this study.
‡ Confirmed using an in-house WB test.
ND = not determined.

positive only by CLEIA, one, seven, and eight plasma samples were positive by LIPS for antibodies against Gag, Tax, and Env, respectively, for 36 plasma samples in Group III; however, there were no positive results for the 14 plasma samples in Group V (Table 1). By LIPS in Group III, one plasma sample (Fig. 2B, double asterisks) exhibited positive responses against Gag and Tax. Other positive plasma samples in Group III exhibited responses against only a single antigen, either Tax or Env. The antibody responses in Group III did not reach the maximum level of those observed in Groups II and IV. According to the criteria of WB indeterminate, the weak responses detected in Group III by LIPS would be considered "indeterminate." Among them, one plasma sample (Fig. 2B, section symbol) tested positive in the additional WB. In Group V, one plasma sample tested positive in the additional IF test, although no antigen reacted with this plasma sample in LIPS (Fig. 2B, dagger). Among the 26 plasma samples in Group VI, one exhibited antibody responses against both Gag and Env (Fig. 2B, double dagger; and Sample Identifier VI-10). The intensity of the luciferase signal for this plasma sample was almost equivalent to that of the plasma samples in Groups II and IV by LIPS for Env, whereas the antibody response against Gag was relatively low. Previously and in this study period, donor VI-10 tested positive for HTLV-1 by CLEIA screening (see Materials and Methods), and this donor tested positive by LIPS for antibodies against both Gag and Env and tested positive in the additional IF test; thus, this donor was probably infected with HTLV-1, although the donor was indeterminate according to the WB test.

Detection of an anti-HBZ response

Recently, HBZ antibody responses were reported for the first time in both asymptomatic HTLV-1 carriers and patients with ATL or HAM/TSP in two cohorts that comprised multiple ethnicities other than Japanese.[11] We also examined the test plasma samples collected in Japan by LIPS for antibodies against HBZ. Among 114 HTLV-1 screening–positive plasma samples, we detected a single case of HBZ positivity in Group IV (Fig. 2B and Sample Identifier IV-8 in Fig. 3A). We confirmed the presence of anti-HBZ in this plasma sample using an in-house WB test with a human 293T cell lysate that transiently expressed HBZ proteins because no commercial tests are available for detecting HBZ antibodies. As shown in Fig. 3A, Plasma Sample IV-8, but not plasma samples from Group I (I-24 and I-25), exhibited a specific band against wild-type and myc-His–tagged HBZ proteins, HBZRLuc, and RLucHBZ with the appropriate estimated molecular weight (Fig. 3A, Lanes 2-5). This is the first identification of an anti-HBZ–positive blood donor in Japan. Plasma Sample IV-8 exhibited consistently high luciferase activities for the antibody responses against all three other antigens in our LIPS test

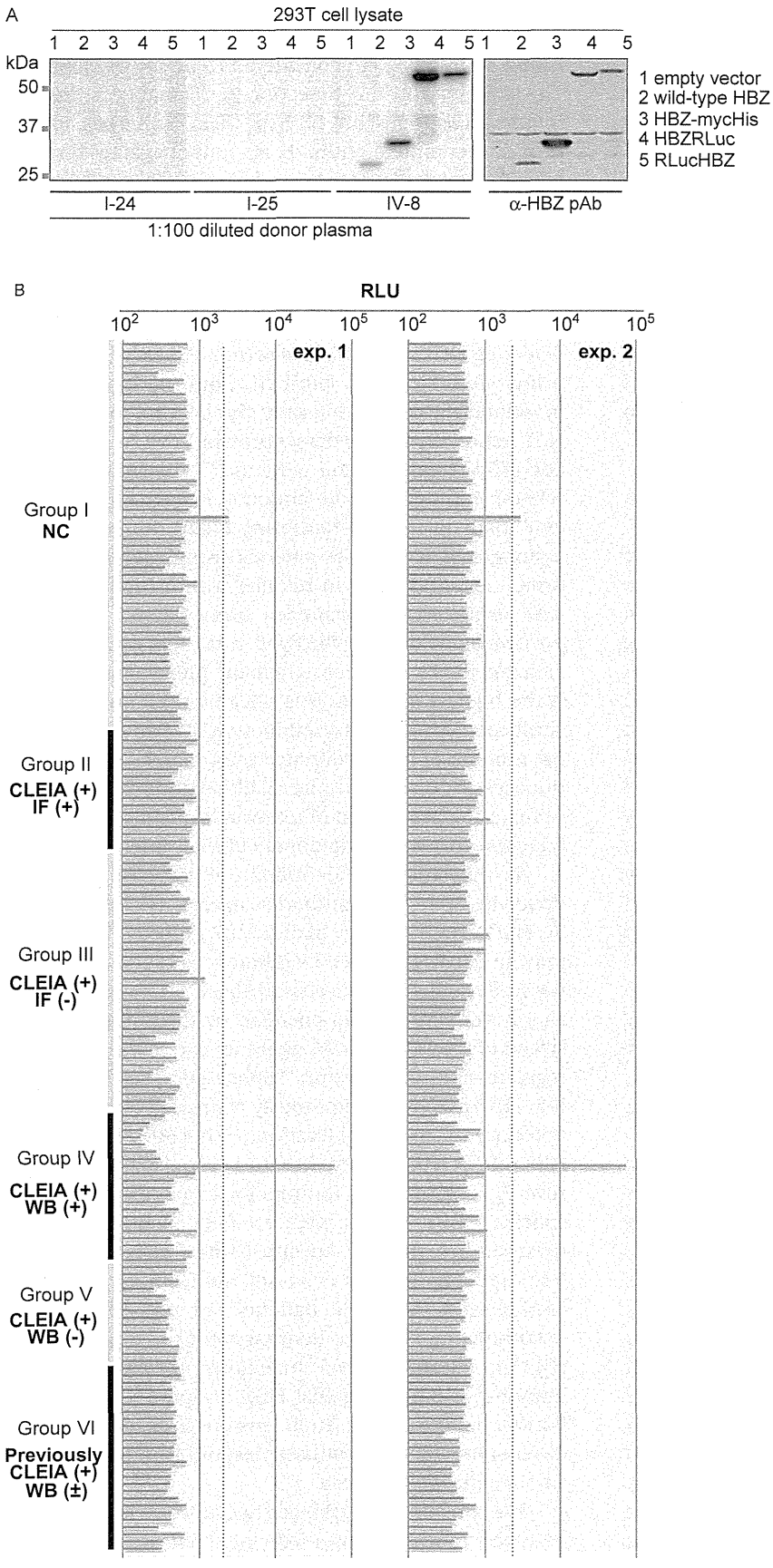

Fig. 3. Characterization of antibody responses against HBZ. (A) Immunoblot analysis against HBZ proteins identified in plasma samples by LIPS. Human 293T cell lysates transfected with an empty vector (Lane 1), wild-type HBZ expression vector (Lane 2), Myc-His-tagged HBZ expression vector (Lane 3), HBZRLuc expression vector (Lane 4), or RLucHBZ expression vector (Lane 5) were analyzed by SDS-PAGE and probed with 1:100-diluted plasma from donors, as indicated by their identifier numbers (I-24, I-25, and IV-8) or with an anti-HBZ rabbit polyclonal antibody (right). (B) Antibody responses against RLucHBZ protein were measured on a separate day by LIPS (Experiments 1 and 2). RLU, measured for 1 second; dotted lines = cutoff values (2071 in Experiment 1 and 2308 in Experiment 2).

(Fig. 2B). We observed that several other plasma samples had relatively strong responses by LIPS for three antigens, that is, Gag, Tax, and Env, in Groups II and IV, whereas they did not bind to the HBZ antigen, except for Plasma Sample IV-8. The frequency of the HBZ antibody was 0.88% (1/114) among the screening-positive donors and 2.63% (1/38) among the confirmatory test–positive donors. Enose-Akahata and coworkers[11] reported that 10.34% (15 in 145) of asymptomatic HTLV-1 carriers exhibited antibody responses against the HBZ protein. To examine whether the low frequency of antibody responses against the HBZ protein in our study was attributable to the C-terminus *Renilla* luciferase fusion structure of our HBZ antigen, that is, HBZRLuc, we analyzed the same test plasma samples using RLucHBZ, where the order of *Renilla* luciferase and HBZ was the same as that reported by Enose-Akahata and coworkers.[7] As shown in Fig. 3B we found that Plasma Sample IV-8 tested positive and exhibited the same high luciferase activity as that detected in tests using HBZRluc. In addition, another positive plasma sample in Group I, that is, I-25, tested negative by CLEIA screening, although the RLU value was much lower than that

of IV-8. To exclude the possibility that the antibody response of I-25 against RLucHBZ was caused by contamination during handling, we repeated the same LIPS test on another day and obtained the same results (Experiment 2 in Fig. 3B). There was no specific signal for the I-25 plasma sample in the immunoblot analysis against the four HBZ proteins (Fig. 3A). Therefore, we consider that the screening-negative plasma sample, I-25, contained antibodies that could weakly bind to a nonlinear epitope in the RLucHBZ antigen but not in the HBZRLuc antigen. These results indicate that the HBZRLuc antigen did not have an impaired capacity for binding HTLV-1–induced antibodies but the structure of HBZRLuc led to a greater specificity. We conclude that the frequency of asymptomatic HTLV-1 carriers who retain anti-HBZ responses in Japan is lower than that in other endemic areas.

DISCUSSION

To explore more reliable tests to identify asymptomatic HTLV-1 carriers among blood donors, we reevaluated two confirmatory tests for HTLV-1 antibodies at our blood center. The LIPS test results for antibodies against the Gag and Env proteins in Groups II and IV were perfectly consistent with those of our previous (IF in Group II) and present (WB in Group IV) HTLV-1 confirmatory test results. These results indicate that the validity of the positive results obtained with both the confirmatory tests used at JRC was further assured using an independent antibody test, that is, LIPS tests. In confirmatory test–negative samples from Groups III and V, LIPS did not identify any plasma samples that were positive for both the Env and the Gag antibodies, indicating that the specificity of both confirmatory tests is equivalent. However, we observed many other types of positive responses via LIPS in Group III, which suggests a particular property of IF in antibody detection. It is likely that some of these antibody responses would be categorized as "indeterminate" in WB, which remains to be fully characterized to assess HTLV-1 confirmatory tests.

Interestingly, our results slightly disagreed with those reported previously, where only LIPS for antibodies against Gag but not Env exhibited 100% positivity in asymptomatic HTLV-1 carriers.[4,7] In our study, all the plasma samples that tested positive in confirmatory tests exhibited unambiguously strong antibody responses against Env (Fig. 2). We assume that the tertiary structure of Env antigens in the Env–*Renilla* luciferase fusion protein in our LIPS was the main contributor to this improvement. This discrepancy may be explained by the different ethnicities of the participants and different distribution of human leukocyte antigen types. The ethnicities of the archived samples and cohorts used in previous studies were mainly Caucasian, African-descent, and Hispanic (Jamaican).[4,7] Our test samples were collected from donors who donated their blood in the Kinki area, which is in the middle part of the Japanese Main Island, and they were considered to be mostly Japanese. The superior anti-Env detection performance is the most important aspect of our LIPS for HTLV-1 analysis because zero or incomplete antibody responses against Env proteins frequently lead to WB-indeterminate results in confirmatory tests.[12-14]

During the screening of donated blood, the most severe issue when determining the HTLV-1 infection status is the lack of gold standard tests, such as the highly sensitive nucleic acid amplification test (NAT) used for detecting HIV-1 and HIV-2 in serum. However, even when using genomic DNA purified from peripheral blood mononuclear cells to measure the proviral load, HTLV-1 NAT frequently fails to detect proviral DNA in asymptomatic HTLV-1 carriers and patients.[15-18] To understand the relationship between the antibody response profiles and viral loads of HTLV-1–harboring blood donors, we have commenced large-scale analysis using several antibody tests, including LIPS, in parallel with a highly sensitive NAT using archived samples from HTLV-1 screening–positive blood donors who lived in the Tokyo metropolitan area and the Kyusyu area, where the prevalence of HTLV-1 is the highest in Japan. It is obvious that more accurate confirmatory tests or a combination of tests would reduce the number of indeterminate cases, thereby reducing the unnecessary disqualification of blood donors and contributing to the prevention of unaware transmission by notifying the corresponding donors of their infection status.

In this study, we identified the first case of a blood donor in Japan with antibodies against HBZ (Figs. 2 and 3). The lower frequency of anti-HBZ detected by our LIPS may be partly explained by differences in the ethnicity of the study subjects, as discussed above. HBZ was identified as a novel viral protein encoded by the complementary strand of the HTLV-1 RNA genome, and it was thought to regulate viral transcription.[19] Subsequent studies showed that HBZ mRNA is ubiquitously expressed in all ATL cells and supports their proliferation.[20,21] In HAM/TSP patients, HBZ mRNA is correlated with the proviral load and disease severity.[22] From an immunologic perspective, HBZ-specific CD8+ T cells were recently identified.[21,23,24] In these studies, the HBZ-specific CD8+ T cells were able to lyse naturally infected cells isolated from asymptomatic carriers and HAM/TSP patients but not ATL patients. Accumulating evidence demonstrates the importance of HBZ in natural HTLV-1 infections; however, humoral immune responses against HBZ are poorly understood. Further epidemiologic studies are required to confirm our observations of HBZ antibody responses in blood donors who are mostly Japanese.

We consider that LIPS has two advantages as an antibody test in transfusion medicine. First, we were able to detect structure-specific antibodies by LIPS without cell

fixation. This feature is particularly useful in confirmatory tests because it complements WB, which only detects the linear epitopes of an antigen. Second, we were able to establish a new test or modify the antigens very easily when we performed the HBZ tests because LIPS does not require the purification of antigens or any secondary antibodies. Only amino acid sequences of the antigens involved are required to implement a new test. This advantage is particularly useful when detecting antibodies against newly emerging infectious diseases, as performed recently in animals[25] and human populations.[26] It would also allow us to expand the existing tests easily by adding new antigens, such as those of HTLV-2. To evaluate the capability of LIPS for detecting antibodies that are critical for blood screening, we must further examine whether LIPS tests can be easily automatized, in addition to testing their sensitivity, specificity, and cost.

ACKNOWLEDGMENTS

We thank Mr Sakamoto and Mr Horikawa at our blood center for preparing the test plasma samples and for helping with data analysis and Ms Tada, Ms Yoshimura, and Mr Gen for their assistance in the IF and WB tests.

CONFLICT OF INTEREST

The authors have disclosed no conflicts of interest.

REFERENCES

1. Inaba S, Sato H, Okochi K, et al. Prevention of transmission of human T-lymphotropic virus type 1 (HTLV-1) through transfusion, by donor screening with antibody to the virus. One-year experience. Transfusion 1989;29:7-11.
2. Thorstensson R, Albert J, Andersson S. Strategies for diagnosis of HTLV-I and -II. Transfusion 2002;42:780-91.
3. Burbelo PD, Ching KH, Mattson TL, et al. Rapid antibody quantification and generation of whole proteome antibody response profiles using LIPS (luciferase immunoprecipitation systems). Biochem Biophys Res Commun 2007;352: 889-95.
4. Burbelo PD, Meoli E, Leahy HP, et al. Anti-HTLV antibody profiling reveals an antibody signature for HTLV-I-associated myelopathy/tropical spastic paraparesis (HAM/TSP). Retrovirology 2008;5:96.
5. Zhao T, Yasunaga J, Satou Y, et al. Human T-cell leukemia virus type 1 bZIP factor selectively suppresses the classical pathway of NF-kappaB. Blood 2009;113:2755-64.
6. Arnold J, Yamamoto B, Li M, et al. Enhancement of infectivity and persistence in vivo by HBZ, a natural antisense coded protein of HTLV-1. Blood 2006;107:3976-82.
7. Enose-Akahata Y, Abrams A, Johnson KR, et al. Quantitative differences in HTLV-I antibody responses: classification and relative risk assessment for asymptomatic carriers and ATL and HAM/TSP patients from Jamaica. Blood 2012; 119:2829-36.
8. Walter P, Johnson AE. Signal sequence recognition and protein targeting to the endoplasmic reticulum membrane. Annu Rev Cell Biol 1994;10:87-119.
9. Martoglio B, Dobberstein B. Signal sequences: more than just greasy peptides. Trends Cell Biol 1998;8:410-5.
10. Martoglio B, Graf R, Dobberstein B. Signal peptide fragments of preprolactin and HIV-1 p-gp160 interact with calmodulin. EMBO J 1997;16:6636-45.
11. Enose-Akahata Y, Abrams A, Massoud R, et al. Humoral immune response to HTLV-1 basic leucine zipper factor (HBZ) in HTLV-1-infected individuals. Retrovirology 2013; 10:19.
12. Lu SC, Chen BH. Seroindeterminate HTLV-1 prevalence and characteristics in blood donors in Taiwan. Int J Hematol 2003;77:412-3.
13. Berini CA, Susana Pascuccio M, Bautista CT, et al. Comparison of four commercial screening assays for the diagnosis of human T-cell lymphotropic virus types 1 and 2. J Virol Methods 2008;147:322-7.
14. Filippone C, Bassot S, Betsem E, et al. A new and frequent human T-cell leukemia virus indeterminate Western blot pattern: epidemiological determinants and PCR results in central African inhabitants. J Clin Microbiol 2012;50:1663-72.
15. Manns A, Miley WJ, Wilks RJ, et al. Quantitative proviral DNA and antibody levels in the natural history of HTLV-1 infection. J Infect Dis 1999;180:1487-93.
16. Etoh K, Yamaguchi K, Tokudome S, et al. Rapid quantification of HTLV-I provirus load: detection of monoclonal proliferation of HTLV-I-infected cells among blood donors. Int J Cancer 1999;81:859-64.
17. Iwanaga M, Watanabe T, Utsunomiya A, et al. Human T-cell leukemia virus type I (HTLV-1) proviral load and disease progression in asymptomatic HTLV-1 carriers: a nationwide prospective study in Japan. Blood 2010;116: 1211-9.
18. Waters A, Oliveira AL, Coughlan S, et al. Multiplex real-time PCR for the detection and quantitation of HTLV-1 and HTLV-2 proviral load: addressing the issue of indeterminate HTLV results. J Clin Virol 2011;52:38-44.
19. Gaudray G, Gachon F, Basbous J, et al. The complementary strand of the human T-cell leukemia virus type 1 RNA genome encodes a bZIP transcription factor that down-regulates viral transcription. J Virol 2002;76:12813-22.
20. Satou Y, Yasunaga J, Yoshida M, et al. HTLV-I basic leucine zipper factor gene mRNA supports proliferation of adult T cell leukemia cells. Proc Natl Acad Sci U S A 2006;103: 720-5.
21. Hilburn S, Rowan A, Demontis MA, et al. In vivo expression of human T-lymphotropic virus type 1 basic leucine-zipper protein generates specific CD8+ and CD4+ T-lymphocyte responses that correlate with clinical outcome. J Infect Dis 2011;203:529-36.
22. Saito M, Matsuzaki T, Satou Y, et al. In vivo expression of the HBZ gene of HTLV-1 correlates with proviral load,

inflammatory markers and disease severity in HTLV-1 associated myelopathy/tropical spastic paraparesis (HAM/TSP). Retrovirology 2009;6:19.
23. Suemori K, Fujiwara H, Ochi T, et al. HBZ is an immunogenic protein, but not a target antigen for human T-cell leukemia virus type 1-specific cytotoxic T lymphocytes. J Gen Virol 2009;90:1806-11.
24. Macnamara A, Rowan A, Hilburn S, et al. HLA class I binding of HBZ determines outcome in HTLV-1 infection. PLoS Pathog 2010;6:e1001117.
25. Burbelo PD, Dubovi EJ, Simmonds P, et al. Serology-enabled discovery of genetically diverse hepaciviruses in a new host. J Virol 2012;86:6171-8.
26. Burbelo PD, Ching KH, Esper F, et al. Serological studies confirm the novel astrovirus HMOAstV-C as a highly prevalent human infectious agent. PLoS ONE 2011;6:e22576.

Arch Virol (2014) 159:1849–1856
DOI 10.1007/s00705-014-2099-y

BRIEF REPORT

Development of T cell lymphoma in HTLV-1 bZIP factor and Tax double transgenic mice

Tiejun Zhao · Yorifumi Satou · Masao Matsuoka

Received: 13 January 2014 / Accepted: 22 April 2014 / Published online: 13 May 2014

Abstract Adult T-cell leukemia (ATL) is an aggressive T-cell malignancy caused by human T-cell leukemia virus type 1 (HTLV-1). ATL cells possess a CD4+ CD25+ phenotype, similar to that of regulatory T cells (Tregs). Tax has been reported to play a crucial role in the leukemogenesis of HTLV-1. The HTLV-1 bZIP factor (HBZ), which is encoded by the minus strand of the viral genomic RNA, is expressed in all ATL cases and induces neoplastic and inflammatory disease *in vivo*. To test whether HBZ and Tax are both required for T cell malignancy, we generated HBZ/Tax double transgenic mice in which HBZ and Tax are expressed exclusively in CD4+ T cells. Survival was much reduced in HBZ/Tax double-transgenic mice compared with wild type littermates. Transgenic expression of HBZ and Tax induced skin lesions and T-cell lymphoma in mice, resembling diseases observed in HTLV-1 infected individuals. However, Tax single transgenic mice did not develop major health problems. In addition, memory CD4+ T cells and Foxp3+ Treg cells counts were increased in HBZ/Tax double transgenic mice, and their proliferation was enhanced. There was very little difference between HBZ single and HBZ/Tax double transgenic mice. Taken together, these results show that HBZ, in addition to Tax, plays a critical role in T-cell lymphoma arising from HTLV-1 infection.

Keywords HTLV-1 · HBZ · Tax · Transgenic mice · Lymphoma

Introduction

Human T-cell leukemia virus type1 (HTLV-1) was the first retrovirus proven to be associated with human disease. Infection with HTLV-1 causes adult T-cell leukemia (ATL) [20, 24]. ATL cells possess a CD4+ CD25+ phenotype, similar to that of regulatory T cells (Tregs). Previous report showed that HTLV-1 provirus is detected mainly in CD4+ memory T cells and Treg cells, suggesting that HTLV-1 favors Treg cells and memory T cells *in vivo* [10, 23, 26].

HTLV-1 encodes several regulatory (*tax* and *rex*) and accessory (*p12*, *p13*, and *p30*) genes in the pX region between the *env* gene and the 3′ Long terminal repeat (LTR) [19]. Another gene, the *HTLV-1 bZIP factor* (*HBZ*), is encoded by the minus strand of the HTLV-1 genome [4]. Among the proteins encoded by these genes, Tax and HBZ play critical roles in ATL [5, 16]. Accumulating evidence shows that Tax can immortalize human primary T cells, enhance viral replication and support cellular proliferation [5]. However, the expression of Tax cannot be detected in approximately 60 % of fresh ATL cells because of genetic and epigenetic changes in the HTLV-1 provirus, which indicated that Tax may not be essential for the development of ATL [15]. We reported previously that HBZ is

Electronic supplementary material The online version of this article (doi:10.1007/s00705-014-2099-y) contains supplementary material, which is available to authorized users.

T. Zhao (✉)
College of Chemistry and Life Sciences, Zhejiang Normal University, 688 Yingbin Road, Jinhua 321004, Zhejiang, China
e-mail: tjzhao@zjnu.cn

T. Zhao · Y. Satou · M. Matsuoka
Laboratory of Virus Control, Institute for Virus Research, Kyoto University, Kyoto, Japan

Present Address:
Y. Satou
Priority Organization for Innovation and Excellence, Center for AIDS Research, Kumamoto University, Kumamoto, Japan

consistently expressed in all ATL cells and promotes proliferation of ATL cells [21]. Non-sense mutations of all HTLV-1 genes except HBZ were generated by APOBEC3G (A3G), suggesting that HBZ is indispensable for the growth and survival of HTLV-1 infected cells [3].

It is noteworthy that Tax and HBZ synergistically regulated the viral transcription and cellular signaling pathways in ATL [29]. HBZ suppressed Tax-mediated HTLV-1 viral transcription through interaction with cAMP response element-binding protein (CREB) [12]. Additionally, HBZ selectively inhibited the classical nuclear factor-κB (NF-κB) pathway which was activated by Tax [27]. We reported that HBZ induced the differentiation of Treg cells by activating the transforming growth factor-β (TGF-β) pathway [28]. Contrariwise, three distinct mechanisms by which Tax suppressed TGF-β–mediated signaling were reported [1, 11, 17]. Taken together, we speculated that the complementary effect of Tax and HBZ on regulating signaling pathways may facilitate better survival of HTLV-1 infected cells and help the cancer cells escape immune attack.

To test the effect of synchronous expression of HBZ and Tax on T cell malignancy in vivo, we generated double transgenic mice expressing HBZ and Tax under the control of the CD4 promoter. In the present study, we found that HBZ/Tax mice have increased memory CD4+ T cells and Foxp3+ Treg cells, resulting in the development of skin lesions and T-cell lymphoma. Both the skin lesions and the lymphoma resemble diseases observed in HTLV-1 infected individuals.

Material and methods

Mice and cell cultures

C57BL/6 J mice were purchased from CLEA Japan. Transgenic HBZ mice expressing HBZ specifically in CD4+ cells have been described elsewhere [22, 25]. Tax single transgenic mice were generated as previously reported [22]. Male HBZ transgenic mice were mated with female Tax transgenic mice, and offspring were typed for the presence of each transgene. Wild-type, HBZ, and Tax single transgenic mice were maintained as controls along with experimental HBZ/Tax transgenic offspring.

All animal experimentation was performed in strict accordance with the Japanese animal welfare bodies, and the Regulation on Animal Experimentation at Kyoto University. The protocol was approved by the Institutional Animal Research Committees of Kyoto University and Zhejiang Normal University. All efforts were made to minimize suffering.

ATL cell lines, ATL-43T and MT-1, were cultured in RPMI-1640 containing 10 % FBS and antibiotics. 293FT cells were maintained as described previously [27].

Semiquantitative RT-PCR and real-time PCR

Total RNA was isolated using Trizol Reagent (Invitrogen) according to the manufacturer's instructions. We reverse-transcribed total RNA into single-stranded cDNA with SuperScript III reverse transcriptase (Invitrogen). For semiquantitative PCR, cDNA was amplified by increasing PCR cycles using forward (F) and reverse (R) primers specific to the target genes. The expression of transgenic genes was quantified by real-time PCR using the Taqman Universal PCR Master Mix (PE Applied Biosystems) according to the manufacturer's instructions.

Lentiviral vector construction and transfection of recombinant lentivirus

We cloned Tax cDNA into a lentiviral vector, pCSII-EF-MCS. Recombinant lentivirus was produced as described. ATL-43T cells were incubated with concentrated vector stocks in the presence of 4 μg/mL polybrene.

Cell isolation and flow cytometric analysis

Murine spleen was carefully crushed to release the lymphocytes. Splenic erythrocytes were eliminated with NH_4Cl. Cells were washed with PBS containing 1 % FBS. After centrifugation, cells were incubated with antibodies for 30 min at 4 °C, and then analyzed with a flow cytometer (BD FACSCanto II, BD Biosciences). For intracellular staining, we used a mouse Foxp3 staining kit according to its protocol (eBioscience).

BrdU staining

In vivo proliferation was measured by BrdU incorporation. BrdU (Nacalai Tesque) was dissolved in PBS (3 μg/ml), and then 200 μl was injected intraperitoneally into transgenic and non-transgenic mice twice a day for three days. BrdU incorporation in CD4+ splenocytes was detected using FITC BrdU Flow Kits (BD Pharmingen) according to the manufacturer's instructions.

Statistical analysis

Statistical analyses were performed using the unpaired student *t* test.